

# Combining the advantages of superconducting $\text{MgB}_2$ and $\text{CaC}_6$ in one material: suggestions from first-principles calculations

Amy Y. Liu<sup>1</sup> and I. I. Mazin<sup>1,2</sup>

<sup>1</sup> *Department of Physics, Georgetown University, Washington, DC 20057-0995*

<sup>2</sup> *Center for Computational Materials Science, Naval Research Laboratory, Washington, DC 20375*

(Dated: September 7, 2018)

We show that a recently predicted layered phase of lithium monoboride,  $\text{Li}_2\text{B}_2$ , combines the key mechanism for strong electron-phonon coupling in  $\text{MgB}_2$  (i.e., interaction of covalent B  $\sigma$  bands with B bond-stretching modes) with the dominant coupling mechanism in  $\text{CaC}_6$  (i.e., interaction of free-electron-like interlayer states with soft intercalant modes). Yet, surprisingly, the electron-phonon coupling in  $\text{Li}_2\text{B}_2$  is calculated to be weaker than in either  $\text{MgB}_2$  or  $\text{CaC}_6$ . We demonstrate that this is due to the accidental absence of B  $\pi$  states at the Fermi level in  $\text{Li}_2\text{B}_2$ . In  $\text{MgB}_2$ , the  $\pi$  electrons play an indirect but important role in strengthening the coupling of  $\sigma$  electrons. Doping  $\text{Li}_2\text{B}_2$  to restore  $\pi$  electrons at the Fermi level is expected to lead to a new superconductor that could surpass  $\text{MgB}_2$  in  $T_c$ .

PACS numbers: 74.25.Jb, 74.25.Kc, 74.70.Ad

## I. INTRODUCTION

The discovery of superconductivity in  $\text{MgB}_2$  at  $T_c = 39$  K led to a new paradigm for achieving high critical temperatures in conventional superconductors, namely strong electron-phonon coupling due to metallization of strong covalent bonds.<sup>1</sup> In  $\text{MgB}_2$ , this is achieved through the interaction of electrons forming covalent B-B bonds in the graphene-like layers with vibrational modes that stretch and compress these bonds.<sup>2</sup> Unfortunately, efforts to find related materials with even higher  $T_c$  have not been fruitful. This is basically because the electronic states that form the covalent bonds in  $\text{MgB}_2$  are quasi two-dimensional, which makes it difficult to enhance their density of states and their coupling to phonons through simple doping.<sup>3</sup> Significant progress may only be possible through the introduction of different types of electronic states at the Fermi level.<sup>3</sup>

The recent discovery of superconductivity in  $\text{CaC}_6$  at  $T_c = 11.5$  K,<sup>4</sup> the highest critical temperature among graphite intercalation compounds (GICs), offers an alternative path to increasing  $T_c$ . Although  $\text{CaC}_6$  is structurally similar to  $\text{MgB}_2$ , it appears that the key electrons and phonons responsible for its superconductivity are distinct from those in  $\text{MgB}_2$ .<sup>5,6</sup> In particular, free-electron-like states that are concentrated in the region between graphene layers dominate the electron-phonon interaction through coupling with soft intercalant modes and with bond-bending modes of the graphene sheet. Incipient lattice instabilities associated with the soft intercalant phonon modes, however, may present obstacles to attaining significantly higher  $T_c$  in GICs.<sup>5,7</sup>

It is intriguing to ask whether the  $\text{MgB}_2$  and  $\text{CaC}_6$  mechanisms for strong electron-phonon coupling can be incorporated into a single compound to create a superconductor with the potential to surpass  $\text{MgB}_2$ . Although neither  $\text{MgB}_2$  nor  $\text{CaC}_6$  can be easily modified so as to incorporate the key electronic and phonon players from the other material, we show here that it is indeed possible

to combine the  $\text{MgB}_2$  and  $\text{CaC}_6$  paradigms in a different material. Such a material has a good chance of exceeding both  $\text{MgB}_2$  and  $\text{CaC}_6$  in terms of  $T_c$ .

The material of interest is a hypothetical layered form of lithium monoboride,  $\text{Li}_2\text{B}_2$ , that recent calculations have predicted to be competitive in energy with known LiB phases.<sup>8,9</sup> The B graphene sheets in  $\text{Li}_2\text{B}_2$  are nearly identical to those in  $\text{MgB}_2$ . At the Fermi level, there are  $\sigma$  bands derived from B  $p_{xy}$  orbitals that form covalent bonds within the layers, as in  $\text{MgB}_2$ , and there are interlayer free-electron-like bands, which we shall call  $\zeta$  bands, as in  $\text{CaC}_6$ . By accident, the B  $p_z$ -derived  $\pi$  states that are present in both  $\text{MgB}_2$  and  $\text{CaC}_6$  are missing at the Fermi level in  $\text{Li}_2\text{B}_2$ . Based on the similarity of the in-plane B physics with  $\text{MgB}_2$ , Kolmogorov and Curtarolo have suggested that this material could be a good superconductor in the mold of  $\text{MgB}_2$ .<sup>8</sup>

In this paper, we analyze the electronic structure of  $\text{Li}_2\text{B}_2$  and show that the electron-phonon interaction has sizable contributions not only from the  $\sigma$  bands that dominate the coupling in  $\text{MgB}_2$ , but also from the interlayer  $\zeta$  bands, which are the key players in  $\text{CaC}_6$ . Surprisingly, the total electron-phonon coupling in  $\text{Li}_2\text{B}_2$  is found to be weaker than in either of the other two materials. We show that this is precisely because of the missing  $\pi$  electrons at the Fermi level. Though the  $\pi$  bands in  $\text{MgB}_2$  and  $\text{CaC}_6$  give only moderate contributions to the electron-phonon coupling,  $\pi$  electrons can indirectly strengthen the coupling of  $\sigma$  electrons with B bond-stretching phonon modes through screening. Doping  $\text{Li}_2\text{B}_2$  to add  $\pi$  sheets to the Fermi surface would enhance the  $\sigma$  contribution to the electron-phonon coupling, as well as add a modest  $\pi$  contribution. While a relatively low  $T_c$  is predicted for pristine  $\text{Li}_2\text{B}_2$ , an appropriately doped material could have a  $T_c$  higher than even  $\text{MgB}_2$ .

## II. CALCULATIONAL METHODS

Our analysis is based on density functional calculations. The electronic structure was calculated using the WIEN2K general potential LAPW code,<sup>10</sup> with the GGA functional in the PBE form.<sup>11</sup> Local orbitals were added to relax the remaining linearization error and APW orbitals were used to improve the convergence with respect to the cutoff parameter  $RK_{\max}$ . In most calculations  $RK_{\max} = 7$  was used, except for the convergence tests with  $RK_{\max} = 8$ . Up to 918 irreducible  $\mathbf{k}$ -points were used ( $32 \times 36 \times 16$ ). The phonon spectrum and electron-phonon coupling functions were calculated using the linear-response method<sup>12</sup> within the local density approximation. Norm-conserving pseudopotentials<sup>13</sup> were used, with a plane-wave cutoff of 50 Ry. The dynamical matrix was calculated on a grid of  $6 \times 6 \times 2$  phonon wavevectors  $\mathbf{q}$  in the Brillouin zone and Fourier interpolated to denser meshes for calculation of the phonon density of states (DOS). For calculation of the electron-phonon matrix elements, the electronic states were sampled on grids of  $36 \times 36 \times 12$   $\mathbf{k}$ -points in the Brillouin zone.

## III. RESULTS AND DISCUSSION

The structure of the hypothetical layered compound  $\text{Li}_2\text{B}_2$ , first proposed in Ref. 8 (in which it is called MS2), consists of honeycomb B sheets, each surrounded above and below by layers of Li on a triangular lattice. There is a horizontal shift between neighboring Li-B-Li sandwich units, leading to an ABAB... stacking sequence of the Li-B-Li trilayer units. While we find that the optimized structural parameters, particularly the interlayer distances, are sensitive to the details of the electron-ion potential and to the exchange-correlation functional, the band structures calculated within the different approximations are very similar. For the results presented here, we have fixed the structural parameters to the optimized values reported in Ref. 8.

The band structure of  $\text{Li}_2\text{B}_2$  near the Fermi level is shown in Fig. 1. As expected, the  $\sigma$  (blue) and  $\pi$  (green) states are derived primarily from in-plane B  $p_{x,y}$  and out-of-plane B  $p_z$  orbitals, respectively. The  $\zeta$  bands (magenta) have substantial Li  $sp$  and B  $p_z$  character. The charge density of the  $\zeta$  electrons, plotted in Fig. 2, is concentrated in the region between Li-B-Li trilayer units, though hybridization with B  $p_z$  orbitals is evident. This is similar to the character of  $\zeta$  bands in GICs.<sup>5,14,15</sup> The Fermi level in  $\text{Li}_2\text{B}_2$  lies at the crossing of the  $\pi$  and  $\pi^*$  bands at K, reminiscent of pure graphite. Note, however, that in graphite, the coincidence of the Fermi level with the  $\pi$ - $\pi^*$  crossing is mandated by the absence of other bands near  $E_F$ , while in  $\text{Li}_2\text{B}_2$ , it is accidental. (Expanding  $c/a$  by  $\sim 10\%$ , for example, moves the  $\pi$ - $\pi^*$  crossing away from the Fermi level by more than 0.5 eV.) Compared to pure graphite, the presence of Li atoms between

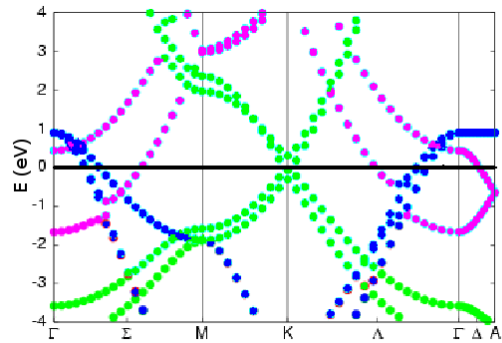


FIG. 1: (Color online)  $\text{Li}_2\text{B}_2$  band structure near the Fermi level ( $E_F = 0$ ). The  $\sigma$ ,  $\pi$ , and  $\zeta$  bands are plotted with blue, green, and magenta symbols, respectively.

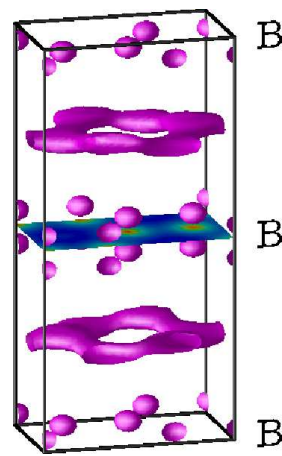


FIG. 2: (Color online) Isosurface of  $\text{Li}_2\text{B}_2$  charge density corresponding to the  $\zeta$  state near the Fermi level, half way between the  $\Gamma$  and A points. The top, center, and bottom plane in the figure contain honeycomb sheets of B. The charge density in the center B plane is shown. Two Li layers lie between each pair of B sheets. The  $\zeta$  states are primarily concentrated in the interlayer region, but have some B  $p_z$  character as well.

the B-based graphene sheets i) makes the  $\pi$  bands more 3D and lowers their energy relative to the  $\sigma$  bands, and ii) lowers the  $\zeta$  bands due to the attractive ionic potential in the interlayer region where the electronic charge in the  $\zeta$  bands is concentrated.<sup>6,14</sup> With these relative shifts in the bands, the  $\sigma$  bands, which are completely filled in pure graphite, become partially occupied in  $\text{Li}_2\text{B}_2$ , while the  $\zeta$  bands, which are unoccupied in graphite, cross the Fermi level in  $\text{Li}_2\text{B}_2$ . Hence  $\text{Li}_2\text{B}_2$  can be viewed as a self-doped analog to pure graphite, with holes in the  $\sigma$  bands exactly compensated by electrons in the  $\zeta$  band. In contrast, in  $\text{CaC}_6$  the  $\pi^*$  band is partially occupied as well.

In comparing the band structures of  $\text{Li}_2\text{B}_2$  and  $\text{MgB}_2$ , which both have B honeycomb sheets separated by “intercalant” layers that donate one electron per B site, key differences in the relative energies of the different types

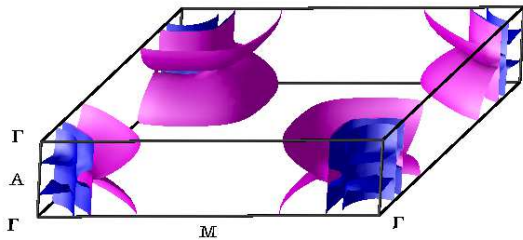


FIG. 3: (Color online) Fermi surface of  $\text{Li}_2\text{B}_2$ . The cylindrical sheets centered on the  $\Gamma$ -to-A line arise from the 2D  $\sigma$  bands, while the ellipsoids are due to free-electron-like  $\zeta$  bands.

of bands can be attributed to the difference in the separation between B layers. With two Li layers between B sheets in  $\text{Li}_2\text{B}_2$ , the B-B interlayer distance in  $\text{Li}_2\text{B}_2$  (5.4 Å) is significantly larger than in  $\text{MgB}_2$  (3.5 Å). This makes the  $p_{xy}$ -derived  $\sigma$  bands more 2D in  $\text{Li}_2\text{B}_2$ , but has little effect on their in-plane dispersion. As in  $\text{MgB}_2$ , these bands give rise to nearly cylindrical hole sheets of the Fermi surface surrounding the  $\Gamma$  to A line. As can be seen in the Fermi surface plotted in Fig. 3, there are two nearly degenerate pairs of  $\sigma$  cylinders. The larger separation between B planes also causes the B  $p_z$ -derived  $\pi$  bands to be more 2D in  $\text{Li}_2\text{B}_2$  and raises them in energy so that the  $\pi^*$  band that is partially occupied in  $\text{MgB}_2$  becomes unoccupied (and just touches  $E_F$  at certain points in the Brillouin zone). The Fermi surface due to the  $\pi$  bands thus disappears in  $\text{Li}_2\text{B}_2$ . On the other hand, the free-electron-like  $\zeta$  bands, which are unoccupied in  $\text{MgB}_2$ , drop in energy when the interlayer distance is increased since there is a larger interlayer volume available for the electrons to occupy.<sup>6,16</sup> In  $\text{Li}_2\text{B}_2$ , the  $\zeta$  bands produce a slightly squashed ellipsoidal Fermi surface around  $\Gamma$ , with a smaller effective mass for motion along the  $z$  direction than in the plane. These ellipsoids are huge compared to the small  $\zeta$  balls in the  $\text{CaC}_6$  Fermi surface,<sup>6</sup> even though  $\text{CaC}_6$  has the most occupied  $\zeta$  band among all GICs.<sup>14</sup>

The topological simplicity of the Fermi surface of  $\text{MgB}_2$ , in which sheets of the Fermi surface corresponding to bands of different character are widely separated in reciprocal space, is lost in  $\text{Li}_2\text{B}_2$ . Not only do the  $\zeta$  ellipsoids cross all four  $\sigma$  cylinders, they also cross each other. At all of these crossings, there is only weak hybridization between the bands. The multiple crossings between sheets of the Fermi surface arising from bands of different character, along with the presence of bands that nearly touch the Fermi level, make Brillouin-zone integrations sensitive to  $\mathbf{k}$ -point sampling. This is especially an issue for calculations of the electron-phonon coupling constants, which involve double integrals over the Fermi surface. The quantitative electron-phonon coupling results presented here likely have larger uncertainties than usual but this does not affect the qualitative picture that emerges.

The phonon density of states  $F(\omega)$  and electron-

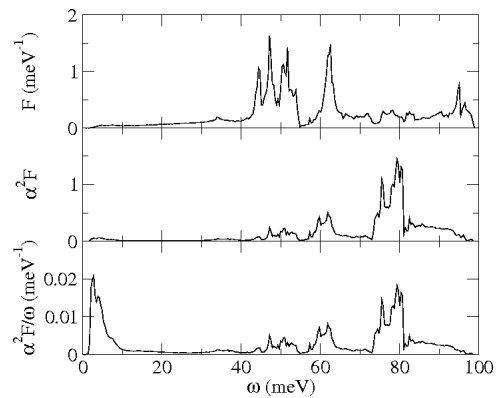


FIG. 4:  $\text{Li}_2\text{B}_2$  phonon density of states  $F(\omega)$ , electron-phonon spectral function  $\alpha^2 F(\omega)$ , and ratio of  $\alpha^2 F$  to frequency  $\omega$ . The electron-phonon coupling constant  $\lambda$ , which is proportional to the inverse-frequency-moment of  $\alpha^2 F$ , has significant contributions from both low-frequency and high-frequency modes.

phonon spectral function  $\alpha^2 F(\omega)$  calculated for  $\text{Li}_2\text{B}_2$  are shown in Fig. 4. The  $E_{2g}$  in-plane bond-stretching B modes that are the key players in superconductivity of  $\text{MgB}_2$  are also important in  $\text{Li}_2\text{B}_2$ , as indicated by the peak in the spectral function near 80 meV. In both materials, these vibrational modes couple strongly to the B  $\sigma$  bands. Given the similarity of the B in-plane physics in the two materials, one expects similar deformation potentials for the  $E_{2g}$  modes.<sup>8</sup> Indeed, our frozen-phonon calculations using LAPW-GGA produce exactly the same deformation potential at  $\Gamma$ : a displacement  $u$  opens a gap  $\Delta\epsilon$  such that  $\Delta\epsilon/u = 26$  eV/Å, precisely the same as found for  $\text{MgB}_2$ .<sup>1</sup> Furthermore, while it is difficult to separate the electronic DOS in  $\text{Li}_2\text{B}_2$  into contributions from different bands, as is routinely done in  $\text{MgB}_2$ , the effective masses derived from the dispersion of the  $\sigma$  bands are within 10% of those in  $\text{MgB}_2$  (the heavy band is 9% heavier and the light band 8% lighter). If the phonon frequencies were the same, one would then expect the net intraband electron-phonon coupling constant for the  $\sigma$  bands,  $\lambda_{\sigma\sigma}$ , to be practically the same as in  $\text{MgB}_2$ . Surprisingly, the phonon frequencies differ considerably. At the zone center, the  $E_{2g}$  phonon frequency of 81 meV in  $\text{Li}_2\text{B}_2$  is significantly higher than the corresponding 67 meV in  $\text{MgB}_2$ ,<sup>2,17</sup> which likely reduces  $\lambda_{\sigma\sigma}$  from  $\approx 1$  to  $\approx 0.6 - 0.7$ .

The hardening of the in-plane B bond-stretching modes in  $\text{Li}_2\text{B}_2$  is related to the loss of  $\pi$  electrons at the Fermi level. The same electron-phonon coupling process that gives rise to superconductivity also leads to electronic screening of phonons. For a zone-center phonon mode, the softening due to screening by metallic electrons is given by

$$\Delta\omega^2 = -4\omega\langle g^2 \rangle N(0), \quad (1)$$

where  $\langle g^2 \rangle$  is a Fermi-surface average of the square of the electron-phonon matrix element  $g$ , and  $N(0)$  is the

electronic DOS at the Fermi level.<sup>2,18</sup> Because the matrix element  $g$  contains a factor of  $1/\sqrt{\omega}$ , the right-hand side of Eq. 1 is independent of the phonon frequency  $\omega$ . In  $\text{MgB}_2$ , both the  $\sigma$  and  $\pi$  electrons participate in screening the bare  $E_{2g}$  phonons. For the  $E_{2g}$  mode in  $\text{MgB}_2$ , it has been estimated that  $\omega^2$  is reduced by about 1500  $\text{meV}^2$  due to screening by  $\pi$  electrons, and by about 2000  $\text{meV}^2$  due to screening by  $\sigma$  electrons, and that the unscreened frequency is  $\omega_0 \approx 90$   $\text{meV}$ .<sup>2</sup> In  $\text{Li}_2\text{B}_2$ , the unscreened frequency and the softening due to  $\sigma$  bands should be roughly the same magnitude as in  $\text{MgB}_2$ , which gives a rough estimate for the screened  $E_{2g}$  phonon frequency of  $\omega = \sqrt{\omega_0^2 - (\Delta\omega^2)_\sigma} \approx 78$   $\text{meV}$ . This is consistent with our actual calculations for  $\text{Li}_2\text{B}_2$ , which yield a frequency of 81  $\text{meV}$  at the zone center. Since only phonons with  $q_{xy} < 2k_F^\sigma$ , where  $k_F^\sigma$  is the radius of the cylindrical  $\sigma$  sheets of the Fermi surface, can couple to  $\sigma$  electrons, softening by  $\sigma$  electrons is only significant when the in-plane component of the phonon wavevector is less than  $2k_F^\sigma$ . Indeed, at the zone boundary, our calculations yield a frequency of 92  $\text{meV}$  for the lowest  $E_{2g}$  branch, consistent with estimates for the unscreened  $E_{2g}$  frequency. While  $\text{Li}_2\text{B}_2$  also has  $\zeta$  electrons, which are not present in  $\text{MgB}_2$ , these are largely localized in the interlayer region and do not couple strongly with the B bond-stretching modes, so they are less effective in screening the  $E_{2g}$  phonons. The harder  $E_{2g}$  frequencies in  $\text{Li}_2\text{B}_2$  compared to  $\text{MgB}_2$  can thus be attributed to the absence of screening by  $\pi$  electrons.

In addition to the high-frequency  $E_{2g}$  peak in the spectral function, there is a low-frequency peak in  $\alpha^2F$  arising from ultrasoft modes that involve rigid shifts of the B planes in the  $z$  direction coupled with both in-plane and out-of-plane motion of the Li atoms. The frequency of these ultrasoft modes is sensitive to calculational details, so at  $\Gamma$ , for example, the harmonic frequency of about 8  $\text{meV}$  obtained in our LDA linear-response calculation is somewhat lower than the estimate of 11  $\text{meV}$  based on force-constant methods using PAW GGA calculations.<sup>8</sup> In any case, these low-frequency normal modes couple with the  $\zeta$  bands, similar to the situation in  $\text{CaC}_6$ , where Ca sliding modes interact strongly with interlayer electrons. Although relatively small, the low-frequency peak in  $\alpha^2F$  gives a similar contribution to the isotropic electron-phonon coupling constant  $\lambda = 2 \int d\omega \alpha^2F/\omega$  as the high-frequency peak (see Fig. 4, bottom panel). The total  $\lambda$  is calculated to be 0.57, with the low-frequency peak contributing about 0.15, and the  $E_{2g}$  peak contributing about 0.2. The logarithmically averaged phonon frequency of  $\omega_{\text{ln}} = \exp[\lambda^{-1} \int d\omega \ln(\omega) \alpha^2F(\omega)/\omega] = 39$   $\text{meV}$ , is well below the average frequency of  $\omega_{\text{ave}} = 59$   $\text{meV}$ , reflecting the importance of the ultrasoft modes.

From the point of view of  $T_c$ , the prospects for  $\text{Li}_2\text{B}_2$  do not look optimistic compared to  $\text{MgB}_2$ , because of both the lack of a  $\pi$ -band contribution to  $\lambda$ , and, perhaps more importantly, the hardening of the key  $E_{2g}$  phonons that are no longer screened by  $\pi$  electrons. Neglecting possi-

ble multiband effects and using the McMillan equation<sup>19</sup> with a typical Coulomb parameter of  $\mu^* = 0.12$ , we estimate  $T_c \approx 7$  K. In comparison, the estimated *isotropic*  $T_c$  in  $\text{MgB}_2$  is 25-30 K. Enhancement of  $T_c$  due to interband anisotropy is expected to be weaker in  $\text{Li}_2\text{B}_2$  since the two groups of electrons contribute more equally to the coupling with phonons. But even if it were of the same order as in  $\text{MgB}_2$ , that is,  $\sim 30\%$  in the effective  $\lambda$ , it would only increase  $T_c$  to about 15 K. The bottom line is that  $\text{Li}_2\text{B}_2$ , if synthesized, might be competitive with  $\text{CaC}_6$  in terms of  $T_c$ , but not with  $\text{MgB}_2$ .

However, that is not the end of the story.

While the *undoped*  $\text{Li}_2\text{B}_2$  is isoelectronic with  $\text{MgB}_2$ , and doping of  $\text{MgB}_2$  is known to unequivocally depress  $T_c$ , the same need not be true for  $\text{Li}_2\text{B}_2$ . Electron doping of  $\text{MgB}_2$  lowers the  $\sigma$  DOS, and hence the electron-phonon coupling, since the bands are not ideally 2D. (Though attempts have been made, hole doping of  $\text{MgB}_2$  has not yet been achieved.) In  $\text{Li}_2\text{B}_2$ , the  $\sigma$  bands are much more 2D, so doping should have little effect on their DOS and electron-phonon coupling. On the other hand, electron doping would start filling the  $\pi$  bands, increasing their DOS. Assuming rigid bands, doping on either B or Li sites could be used to raise the Fermi level by nearly 1 eV without losing the contribution from the  $\sigma$  bands. We estimate that this would increase the  $\pi$ -band DOS to roughly half the value in  $\text{MgB}_2$ . Doping on the Li sites (with Al, Be, Mg, etc.) should yield even higher  $\pi$  DOS, since the extra ionic charge in the Li planes would lower the  $\pi$  bands relative to the  $\sigma$  bands. Experience shows that it is hard to dope more holes into the  $\sigma$  bands than there already are in pure  $\text{MgB}_2$ . Since  $\text{Li}_2\text{B}_2$  starts with more holes in the  $\sigma$  bands than  $\text{MgB}_2$ , it might even be easier to synthesize electron-doped  $\text{Li}_2\text{B}_2$  than the undoped material. Assuming that the  $\pi$  bands in doped  $\text{Li}_2\text{B}_2$  couple with the  $E_{2g}$  modes at about the same level as in  $\text{MgB}_2$ , this additional coupling will soften the  $E_{2g}$  phonons and enhance their coupling with the  $\sigma$  bands, without strongly affecting the coupling of  $\zeta$  bands with soft modes. This is an extremely favorable combination that is likely to have a higher  $T_c$  than  $\text{MgB}_2$ . To a lesser extent the same holds if the accidental alignment of the Fermi level with the  $\pi$ - $\pi^*$  crossing is modified by uniaxial pressure.

While  $\text{Li}_2\text{B}_2$  and related layered lithium borides proposed by Kolmogorov and Curtarolo<sup>8</sup> are only hypothetical materials as yet, their calculations of the Li-B phase diagram have suggested a route for synthesizing these materials using pressure.<sup>9</sup> We have shown that although  $\text{Li}_2\text{B}_2$  seems to combine the key mechanism for strong electron-phonon coupling in  $\text{MgB}_2$  with the dominant coupling mechanism in  $\text{CaC}_6$ , each of which has the highest superconducting transition temperature in its respective class of materials, the transition temperature of  $\text{Li}_2\text{B}_2$  is expected to be lower because of the lack of the seemingly unimportant  $\pi$  electrons at the Fermi level. An appropriately doped version of the material, in which  $\pi$  electrons are restored at the Fermi level, however, could

result in a promising new superconductor that combines the paradigms of  $\text{MgB}_2$  and  $\text{CaC}_6$  in a single material without loss. Further calculations using the virtual crystal approximation or the supercell approximation to explore the quantitative effects of doping on the electron-phonon coupling in this material would be of interest.

### Acknowledgments

We thank L. Boeri, G. Bachelet and O.K. Andersen for useful discussions, and S. Massida and E.K.U. Gross

for sharing with us their work on superconductivity in  $\text{CaC}_6$  prior to publication. One of the authors (I.I.M.) thanks Georgetown University for its hospitality during a sabbatical stay. This work was supported by NSF Grant No. DMR-0210717.

- 
- <sup>1</sup> J. M. An and W.E. Pickett, Phys. Rev. Lett. **86**, 4366 (2001).
  - <sup>2</sup> I.I. Mazin and V.P. Antropov, Physica C, **385**, 49 (2003).
  - <sup>3</sup> W. E. Pickett, cond-mat/0603428.
  - <sup>4</sup> N. Emery, C. Herold, M. d'Astuto, V. Garcia, Ch. Bellin, J. F. Mareche, P. Lagrange, and G. Loupiau, Phys. Rev. Lett. **95**, 087003 (2005).
  - <sup>5</sup> M. Calandra and F. Mauri, Phys. Rev. Lett. **95**, 237002 (2005).
  - <sup>6</sup> I. I. Mazin, L. Boeri, O.V. Dolgov, A.A. Golubov, G.B. Bachelet, M. Giantomassi, and O.K. Andersen, cond-mat/0606404.
  - <sup>7</sup> J. S. Kim, L. Boeri, R. K. Kremer, and F. S. Razavi, cond-mat/0603530.
  - <sup>8</sup> A. N. Kolmogorov and S. Curtarolo, Phys. Rev. B **73**, 180501(R) (2006).
  - <sup>9</sup> A. N. Kolmogorov and S. Curtarolo, cond-mat/0607654.
  - <sup>10</sup> P. Blaha *et al.*, WIEN2k, An Augmented Plane Wave + Local Orbitals Program for Calculating Crystal Properties, Karlheinz Schwarz, Techn. Universität Wien, Austria, 2001
  - <sup>11</sup> J. P. Perdew, K. Burke, and M. Ernzerhof, Phys. Rev. Lett. **77**, 3865 (1996).
  - <sup>12</sup> A. A. Quong and B. M. Klein, Phys. Rev. B **46**, 10734 (1992); A. Y. Liu and A. A. Quong, *ibid* **53**, 7575 (1996).
  - <sup>13</sup> N. Troullier and J. L. Martins, Phys. Rev. B **43**, 1993 (1991).
  - <sup>14</sup> G. Csanyi, P. B. Littlewood, A. H. Nevidomskyy, C. J. Pickard, and B. D. Simons, Nature Phys. **1**, 42 (2005).
  - <sup>15</sup> I. I. Mazin, Phys. Rev. Lett. **95**, 227001 (2005)
  - <sup>16</sup> In  $\text{CaC}_6$  the  $\zeta$  band lies substantially lower than in the isoelectronic  $\text{LiC}_3$  (cf. Ref. 14). This is due entirely to an additional interlayer compression of the  $\zeta$  band in  $\text{LiC}_3$ , due to a smaller  $c/a$  (I.I. Mazin, unpublished).
  - <sup>17</sup> Ref. 8 reports a 4% enhancement of the anharmonic frequency of the  $E_{2g}$  phonon in  $\text{Li}_2\text{B}_2$  compared to  $\text{MgB}_2$ , as opposed to our 21% enhancement of the harmonic frequency. The frozen-phonon in  $\text{MgB}_2$  might indeed be more anharmonic due to the smaller Fermi energy of the  $\sigma$  holes, but anharmonic calculations are known to be exceptionally sensitive to the k-point sampling. Moreover, it has been shown that the frozen-phonon approach, which includes only one-phonon anharmonic effects, severely overestimates the anharmonicity in  $\text{MgB}_2$ , and that harmonic calculations are closer to the real frequencies [M. Lazzeri, M. Calandra, and F. Mauri, Phys. Rev. B **68**, 220509(R) (2003)].
  - <sup>18</sup> C. O. Rodriguez, A. I. Liechtenstein, I. I. Mazin, O. Jepsen, O. K. Andersen, and M. Methfessel, Phys. Rev. B **42**, 2692 (1990).
  - <sup>19</sup> W. L. McMillan, Phys. Rev. **167**, 331 (1968).